

Permeability Measurements of Very Thin Magnetic Film Using a Flexible Microstrip-Line-Type Probe

K. Kusunoki, S. Yabukami*, T. Ozawa*, H. Uetake*, H. Yamada, Y. Miyazawa**, and Y. Shimada***

Sendai National College of Technology, 48 Nodayama, Medeshima-Shiote, Natori 981-1239, Japan

*Tohoku Gakuin University, 1-13-1 Chuo, Tagajo 985-8537, Japan

**Toei Scientific Industrial Company Ltd, 1-101-60 Medeshimadai, Natori 981-1251, Japan

***Graduate School of Engineering, Tohoku University, 6-6-05 Aramaki Aza Aoba, Aoba-ku, Sendai 980-8579, Japan

A highly sensitive probe to measure thin film permeability was developed based on the skin effect. A microstrip-line-type probe on a flexible polyimide substrate was fabricated and placed in contact with a magnetic thin film. The permeability was optimized by the Newton–Raphson method. The permeability of amorphous $\text{Co}_{85}\text{Nb}_{12}\text{Zr}_3$ film (25 mm x 25 mm and 5 nm in thickness) was evaluated using a permeameter. The measured values were in rough agreement with theoretical values based on the Landau–Lifshitz–Gilbert equation and eddy current generation up to 7 GHz. The proposed method shows promise for the measurement of very thin film (less than 10 nm in thickness) because the contact surface between the flexible probe and thin film fits very well, resulting in improvement of the signal-to-noise ratio.

Key words: flexible microstrip-line-type probe, skin effect, permeability, very thin film

1. Introduction

Evaluation of high frequency permeability and gyromagnetic parameters in very thin magnetic films is important because GMR, TMR and other spintronic devices are fabricated from very thin film (film thickness is less than 10 nm). However, almost all permeameters^{1)–3)} require a film thickness of more than 100 nm because the signal-to-noise ratio is limited by the offset between the magnetic thin film and the conductor of a pickup coil or transmission line. Therefore, researchers and engineers deposit a thin film on a microstrip line or a coplanar line for evaluation of gyromagnetic parameters⁴⁾. Thus, they would welcome a permeameter applicable to as-deposited very thin film.

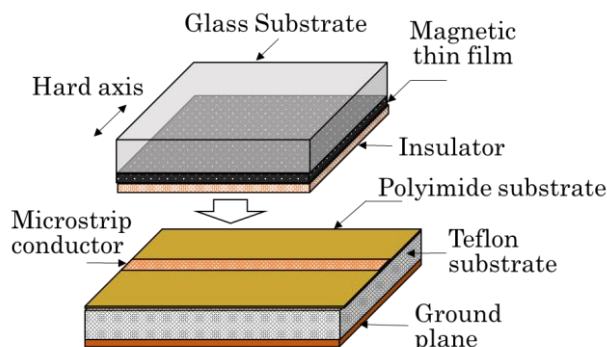
In a previous study, we developed a microstrip-line-type probe whose characteristic impedance was around 50 Ω, including a through hole. We reported that the probe was available for permeability measurement of CoFeB film (0.5 μm in thickness) up to 30 GHz⁵⁾. However, the probe was not always applicable for evaluation of a very thin film (such as that less than 10 nm in thickness) because of the low signal-to-noise ratio.

In the present study, we developed a new probe composed of a straight microstrip line on a flexible polyimide substrate. The flexibility of the probe enables contact between the probe and magnetic thin film which enhances the signal-to-noise ratio.

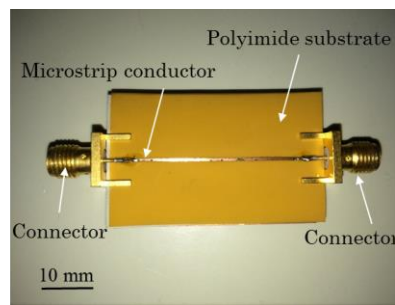
2. Experimental setup

2.1 A new probe and system setup

Fig. 1(a) shows a schematic diagram of the probe and magnetic film. Fig. 1(b) shows a photograph of the probe. The new probe is composed of a straight microstrip conductor (30 mm in length and 0.5 mm in



(a) Schematic diagram of probe and magnetic film



(b) Photograph of the probe

Fig. 1 Schematic diagram and photograph of the probe.

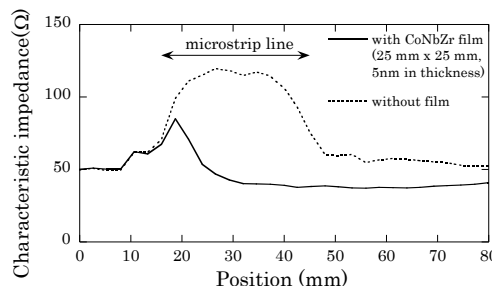


Fig. 2 Characteristic impedance of the probe obtained from time-domain reflectometry (TDR) measurements.

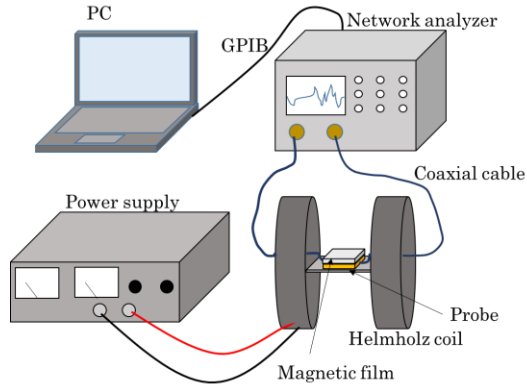


Fig. 3 Schematic diagram of the system setup.

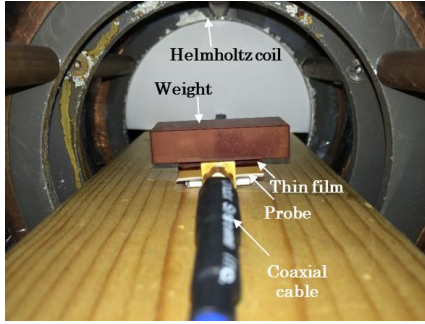


Fig. 4 Photograph of the probe and film.

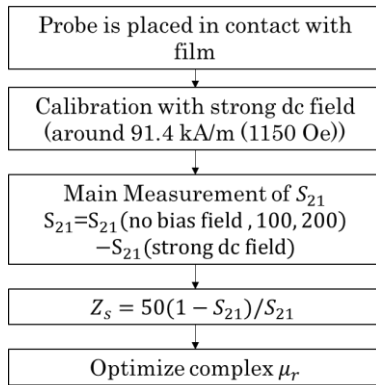


Fig. 5 Flow chart of the permeability measurements.

width) on a polyimide substrate (25 μm in thickness), a Teflon substrate (0.5 mm in thickness), a ground plane, and two connectors. A magnetic thin film coated with photo-resist (about 8 μm in thickness) is in contact with the flexible microstrip conductor. Coaxial cables are connected to a network analyzer. The probe can be easily bent because of the flexibility of the polyimide substrate; therefore, the contact surface between the probe and the thin film fits very well to improve the signal-to-noise ratio.

Fig. 2 shows the characteristic impedance of the probe measured by time domain reflectometry (Agilent Technologies N5227A). The solid line shows the characteristic impedance with amorphous Co₈₅Nb₁₂Zr₃ film (25 mm x 25 mm, 5 nm in thickness), and the dotted line shows that without the film. The characteristic impedance was 40 Ω-80 Ω along the microstrip line. The characteristic impedance was about 110 Ω along the microstrip line without the CoNbZr film. A decrease of the characteristic impedance with the CoNbZr film by about 70 Ω was observed because of the increase of the capacitance. The characteristic

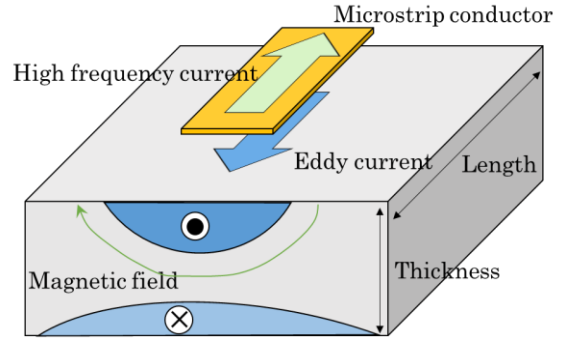


Fig. 6 Schematic diagram of eddy current and magnetic field in a film.

impedance along the microstrip line with the CoNbZr film was not symmetrical, which is because the reflected signal was attenuated by the loss of the CoNbZr film and the multiple reflection.

Fig. 3 shows the system setup, which consists of the probe, a Helmholtz coil, a network analyzer (Agilent Technologies N5227A), a dc power supply (Takasago GPO-60-30), and a personal computer. Fig. 4 shows a photograph of the arrangement of the probe and a magnetic thin film inside a Helmholtz coil. A small weight (about 8 g) was placed on the thin film to achieve contact with the probe conductor, as shown in Fig. 4.

2.2 Optimization of permeability

Fig. 5 shows a flow chart of optimization of permeability. The complex impedance of the magnetic film is transformed from S_{21} using a network analyzer.

Firstly, S_{21} is calibrated by application of a strong dc field (around 91.4 kA/m (1150 Oe)) in the direction of the easy axis to saturate the magnetic film. Secondly, S_{21} is measured without a strong dc field, and then the complex impedance is calculated by equation (1).

$$Z_s = 50(1 - S_{21}) / S_{21} \quad (1)$$

The effect of resistance of the microstrip conductor, as well as that of the outer inductance of the magnetic film, can be eliminated. The S_{21} and Z_s included the multiple reflections in equation (1). Complex permeability is optimized using the Newton-Raphson method⁶⁾ to take the skin effect of the magnetic film into account by using equations (2) - (4),

$$Z_s = \frac{k_s \rho l}{2w} \cot\left(\frac{k_s t}{2}\right) - \frac{k'_s \rho l}{2w} \cot\left(\frac{k'_s t}{2}\right) \quad (2)$$

$$k_s = \frac{(1+j)}{\sqrt{\frac{\rho}{\pi f \mu_r \mu_0}}} \quad (3)$$

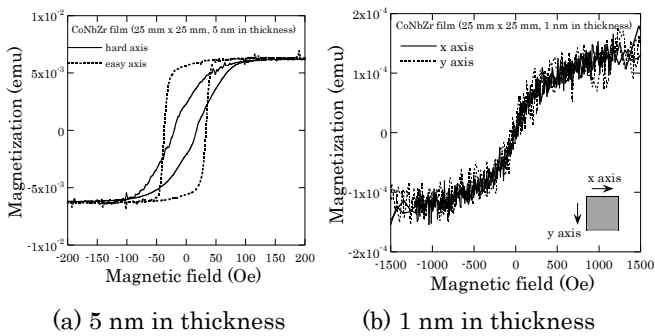
$$k'_s = \frac{(1+j)}{\sqrt{\frac{\rho}{\pi f \mu_r^{ref} \mu_0}}} \quad (4)$$

where ρ is the resistivity of the film, t is the film thickness, l is the microstrip line length, and w is the width of the microstrip conductor, μ_r^{ref} is relative permeability when a strong dc field of 1150 Oe was

applied. Fig. 6 shows a schematic diagram of the current and the magnetic field in the film, and the microstrip conductor. The high frequency current induces a magnetic field in the width direction of the conductor pattern, and the magnetic field and the eddy current are localized in the skin of the magnetic film. The specified permeability in the width direction corresponds to the high frequency impedance while sacrificing applied magnetic field uniformity. In this paper, very thin CoNbZr films (1 nm and 5 nm in thickness) were evaluated as being highly sensitive.

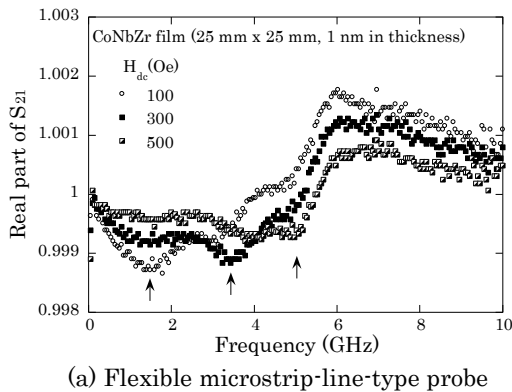
3. Experimental results

Fig. 7 shows the MH curves of CoNbZr film. The film

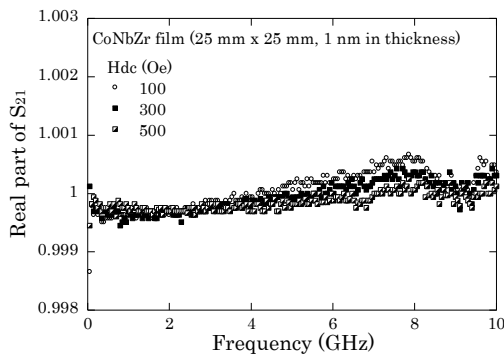


(a) 5 nm in thickness (b) 1 nm in thickness

Fig. 7 MH-curve of the CoNbZr film (25 mm × 25 mm, 5 nm and 1 nm in thickness).



(a) Flexible microstrip-line-type probe

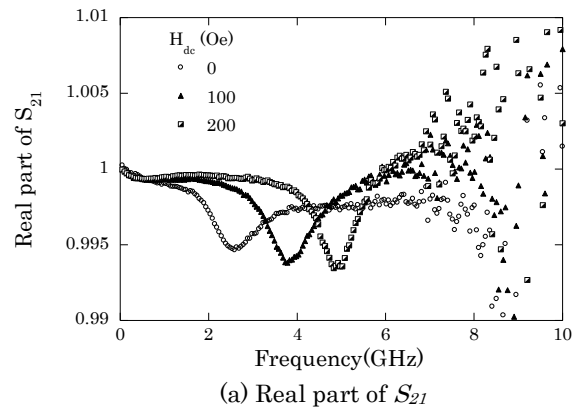


(b) Non-flexible microstrip-line-type probe made of Teflon substrate⁵⁾

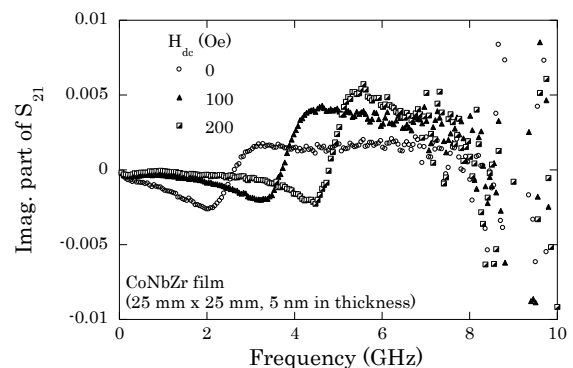
Fig. 8 S_{21} (real part) of the probes when CoNbZr film (25 mm × 25 mm, 1 nm in thickness) is in close contact with the probes (the width of the microstrip conductors was 1 mm). The signal-to-noise ratio of the flexible probe was compared with that of a conventional probe made from a Teflon substrate.

was deposited by RF sputtering. Fig. 7(a) shows the MH curve of CoNbZr film (25 mm × 25 mm and 5 nm in thickness). The dotted line shows the MH curve of the easy axis, and the solid line shows that of the hard axis. The resistivity of the film was about $1.52 \times 10^{-6} \Omega\text{m}$ ($152 \mu\Omega\text{cm}$), which was slightly higher than that of bulky CoNbZr ($120 \mu\Omega\text{cm}$). An anisotropy field of around 70 Oe was observed. The anisotropy field was comparatively larger than that of previous studies^{7),8)}, which is probably because the CoNbZr film was partly crystallized. Fig. 7(b) shows the MH curve of the CoNbZr film (25 mm × 25 mm and 1 nm in thickness). The MH curve was noisy, and visible anisotropy was not always observed. The resistivity of the film was about $1.01 \times 10^{-1} \Omega\text{m}$, which was much higher than that of bulky CoNbZr. The 1 nm thick CoNbZr film was not always a continuous membrane.

Fig. 8 shows the real part of the transmission coefficient (S_{21}) of the probes when the CoNbZr film (25 mm × 25 mm, 1 nm in thickness) was in direct contact with the probe (the width of the microstrip conductors was 1 mm). Fig. 8 (a) shows the S_{21} measured by using the flexible microstrip-line-type probe, and Fig. 8(b) shows the S_{21} measured using the non-flexible microstrip probe⁵⁾ made of Teflon substrate. Bias fields of 100, 300 and 500 Oe were applied along the easy axis. In Fig. 8 (a), small ferromagnetic resonances (arrowed)



(a) Real part of S_{21}



(b) Imaginary part of S_{21}

Fig. 9 S_{21} of the flexible microstrip-line-type probe (the width of the microstrip conductor was 0.5 mm) when CoNbZr film (25 mm × 25 mm, 5 nm in thickness) was in contact with the probe. Bias fields of 0, 100, and 200 Oe were applied along the easy axis. Ferromagnetic resonance shifted as the bias field increased.

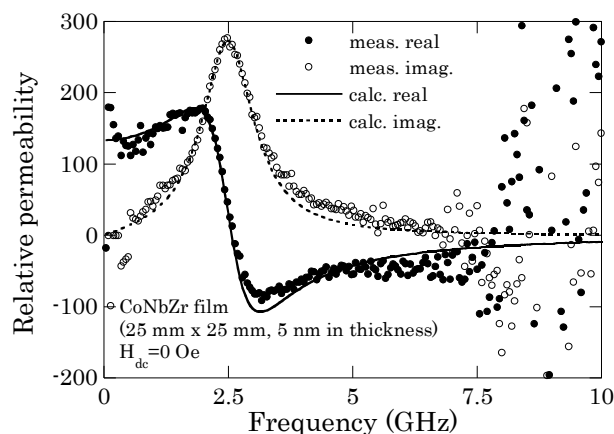
Table 1 Comparison between the probe of Fig. 8 and that of Fig. 9.

Probe	Width of microstrip conductor (mm)	Contact between microstrip conductor and CoNbZr film
Fig. 8	1.0	Direct electrical contact
Fig. 9	0.5	Photo-resist (about 8 μm in thickness) was inserted

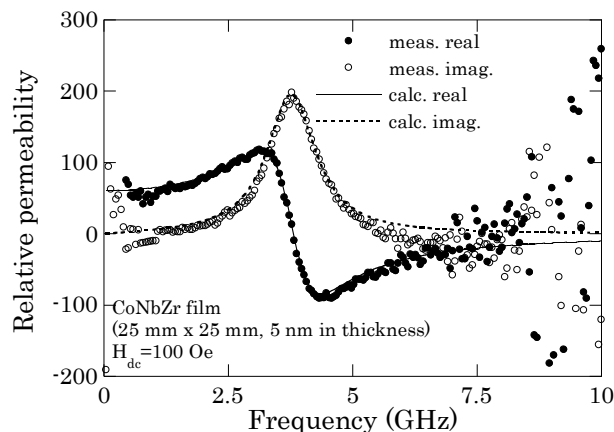
were observed and the resonance frequency shifted as the bias field increased. However, ferromagnetic resonances are not observed in Fig. 8 (b). Therefore, the good contact between the flexible probe and the very thin film enhanced the signal-to-noise ratio.

Fig. 9 shows S_{21} of the flexible probe when the CoNbZr film (25 mm \times 25 mm, 5 nm in thickness) was in contact with the flexible probe. Fig. 9 (a) shows the real part of S_{21} and Fig. 9 (b) shows the imaginary part. No bias field, a 100 Oe bias field and a 200 Oe bias field were applied in the direction of the easy axis. A strong dc field of about 1150 Oe was applied for background measurement. The ferromagnetic resonances were observed, and the resonance frequency was found to shift as bias field increased. The ferromagnetic resonance was observed at about 2.5 GHz without a bias field, which was reasonable as the anisotropy field of 70 Oe. Some non-magnetic resonances were observed over 7 GHz because of the impedance mismatch, and the frequency characteristics differed from those of Fig. 8. Table 1 shows a comparison between the probe of Fig. 8 and that of Fig. 9. The two probes differed in the width of the microstrip conductor and the contact between the microstrip conductor and the CoNbZr film. The different frequency responses were caused by the differences of the characteristic impedances and the current passes between the two probes.

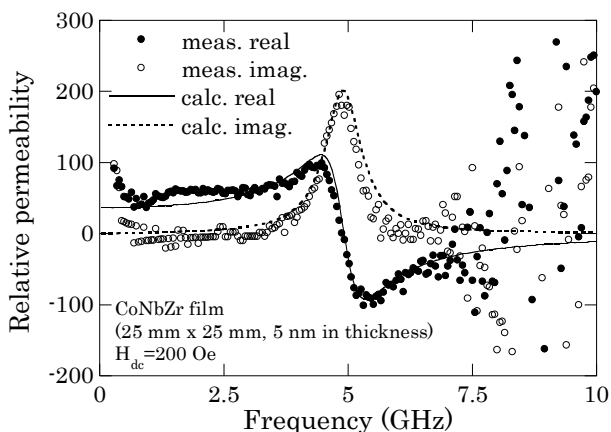
Fig. 10 shows the permeability, which was optimized from S_{21} shown in Fig. 9. Fig. 10 (a) shows the permeability without the bias field, (b) and (c) show the permeability when bias fields of 100 and 200 Oe were applied along the easy axis. The symbols show measured permeability, and the dotted lines and the solid lines show the theoretical permeability based on the Landau–Lifshitz–Gilbert equation and eddy current generation⁹⁾. A g factor of 2.13¹⁰⁾ was used to calculate theoretical permeability. An α (damping factor) of 0.04 was used in order to fit theoretical permeability to measured spectra. The absolute permeability was calibrated by the application of dc magnetic fields in the direction of the easy axis. The measured permeability roughly corresponded to the theoretical permeability up to 7 GHz. Ferromagnetic resonance shifted from 2.5 to 5 GHz as the dc field increased. The microstrip line resonated over 7.5 GHz because of impedance mis-matching. Therefore, the new probe can be useful for measurement of the permeability of very thin film.



(a) No bias field



(b) 100 Oe



(c) 200 Oe

Fig. 10 Hard axis permeability of CoNbZr film (25 mm \times 25 mm, 5 nm in thickness) by using the flexible microstrip-line-type probe. (a) No bias field was applied; (b),(c) bias fields of 100 and 200 Oe were applied to the easy axis.

4. Conclusions

1. A highly sensitive probe was developed to measure very thin film permeability using a straight microstrip line and a flexible substrate.
2. The transmission coefficient (S_{21}) of a CoNbZr film

(25 mm × 25 mm, 1 nm in thickness) was evaluated. Good contact between the flexible probe and magnetic film resulted in enhancement of the signal-to-noise ratio.

3. A CoNbZr film (25 mm × 25 mm, 5 nm in thickness) was evaluated and the measured permeability was in rough agreement with the theoretical permeability up to 7 GHz.

Acknowledgments We would like to thank Mr. Fujita of Japan Science and Technology Bureau for his advice, Dr. Nakai of Industrial Technology Institute, Miyagi Prefectural Government for his help in measurement of MH-curves, and the Machine Shop of Tohoku Gakuin University for help in fabricating the probe. This work was supported in part by the Program for Revitalization Promotion of JST.

References

- 1) P. A. Calcagno, D. A. Thompson: *Rev. Sci. Instrum.*, **46**, 904 (1975).

- 2) M. Yamaguchi, S. Yabukami and K.I. Arai: *IEEE Trans. Magn.*, **32**, 4941 (1996).

- 3) H. B. Weir: *Proc IEEE*, **62**, 33 (1975).

- 4) G. Counil, Joo-Von Kim, T. Devolder, C. Chappert, K. Shigeto and Y. Otani, *J. Appl. Phys.* **95**, 5646 (2004).

- 5) T. Kimura, S. Yabukami, T. Ozawa, Y. Miyazawa, H. Kenju, Y. Shimada: *J. Magn. Soc. Jpn.* **38**, pp. 87-91 (2014).

- 6) W.H. Press, S.A. Teukolsky, W.T. Vetterling and B.P. Flannery: *Numerical Recipes in C (Japanese Edition)*, pp.251–281, (Gijutsu Hyoron sha, Tokyo,1993).

- 7) H. Katada, T. Shimatsu, I. Watanabe, H. Muraoka, Y. Nakamura and Y. Sugita: *J. Magn. Soc. Jpn.*, **24**, 539 (2000).

- 8) M.L. Schneider, A.B. Kos, and T.J. Silva: *Applied Physics Letters*, **85**, 254 (2004).

- 9) Y. Shimada, J. Numazawa, Y. Yoneda and A. Hosono: *J. Magn. Soc. Jpn.*, **15**, 327(1991).

- 10) A. Yoshihara, K. Takanashi, M. Shimada, O. Kitakami and Y. Shimada: *Jpn. J. Appl. Phys.* **33**, 3927 (1994).

Received Dec. 11, 2014; Accepted Mar. 13, 2015